Available online at www.sciencedirect.com
ScienceDirect
International Journal of Heat and Mass Transfer 50 (2007) 1641–1648
International Journal of HEAT and MASS TRANSFER
www.elsevier.com/locate/ijhmt

A modified k–ε turbulence model for the simulation of two-phase flow and heat transfer in condensers

Hong Gang Hu, Chao Zhang *

Department of Mechanical and Materials Engineering, The University of Western Ontario, London, Ont., Canada N6A 5B9

Received 19 February 2006; received in revised form 21 October 2006
Available online 28 December 2006

Abstract

A modified k–ε turbulence model is developed in this study to simulate the gas–liquid two-phase flow and heat transfer in steam surface condensers. A quasi-three-dimensional algorithm is used to simulate the fluid flow and heat transfer in steam surface condensers. The numerical method is based on the conservation equations of mass and momentum for both gas-phase and liquid-phase, and mass fraction conservation equation for non-condensable gases. The numerical simulation of an experimental steam surface condenser has been conducted using the proposed modified k–ε turbulence model. The results obtained from the proposed model agree well with the experimental results and the results also show an obvious improvement in the prediction accuracy comparing with previous results where a constant value for the turbulent viscosity was used.

Keywords: Heat transfer; Numerical simulation; Condenser; Porous medium; Gas–liquid two-phase flow; k–ε turbulence model

1. Introduction

Steam surface condensers are widely used in the power generation industry. And the improvement of the performance of condensers could result in a significant increase in the efficiency and energy saving. Therefore, it is of great importance to understand the fluid flow and heat transfer in condensers in order to improve the design of condensers. However, the experimental method is very expensive and time-consuming. With the development of computer technology, it becomes possible to simulate a complicated fluid flow and heat transfer process by numerical methods. The fluid flow in steam surface condensers is turbulent and multi-phase with distributed flow resistance due to tube bundles. Therefore, a suitable turbulence model for multi-phase flows with distributed flow resistance is necessary in order to simulate the performance of steam condensers more accurately. The numerical simulations of fluid flow and heat transfer in steam surface condensers have been conducted by several researchers [1–8]. However, in these studies, either the turbulent effect was neglected [1], or a constant ratio of the turbulent viscosity to the dynamic viscosity was used [2–6], or a simple algebraic expression was used to determine the turbulent viscosity [7,8]. In the numerical simulation of the two-phase flow with distributed flow resistance in a steam generator conducted by Stosic and Stevanovic [9], the flow was assumed non-viscous and the turbulent effect was indirectly taken into account through friction or drag terms. Therefore, the objectives of this study are to develop a suitable turbulence model for gas–liquid two-phase flows in steam surface condensers where distributed flow resistance exists and valid the proposed turbulence model using experimental data.

The experimental steam surface condenser and experimental data from Al-Sanea et al. [6] and Bush et al. [8] are selected in this study to validate the proposed numerical model. The numerical results obtained by the current numerical model are also compared with the results by using the numerical model with a constant turbulent viscosity.

* Corresponding author.
E-mail address: zhangc@engga.uwo.ca (C. Zhang).

0017-9310/$ - see front matter © 2006 Elsevier Ltd. All rights reserved.
doi:10.1016/j.ijheatmasstransfer.2006.10.031

Nomenclature

A	heat transfer area of a given control volume
A_d	total projected area of droplets in a given control volume
C_1, C_2, C_μ	constants in k–ε model
C_f	interphase friction coefficient
C_{phase}	constant
D	diffusivity of air in steam
D_d	diameter of a droplet
D_e	effective diffusivity of air in steam
D_t	turbulent diffusivity of air in steam
F	force due to flow resistance
f_d	friction factor
g	gravitational acceleration
G	generation of turbulent kinetic energy
k	gas-phase turbulent kinetic energy
$\dot{m}$	vapor condensation rate per unit volume
p	pressure
q''	heat flux
R	source term due to tube bundles
U	velocity magnitude
u	velocity component in x-direction
V	volume
v	velocity component in y-direction
W	source term due to the interphase friction
x	x-coordinate
y	y-coordinate

Greek symbols

α	local porosity
β	volume fraction
ε	dissipation rate of turbulent kinetic energy
μ	laminar dynamic viscosity
μ_e	effective viscosity
μ_t	turbulent viscosity
ρ	density
σ	turbulent Prandtl number
τ	shear stress
ϕ	generalized variable

Subscripts

a	air
g	gas-phase (mixture of vapor and non-condensable gases)
k	parameter for turbulent kinetic energy
l	liquid-phase
m	phase in question (g or l)
t	turbulence
x	parameter in x-momentum equation
y	parameter in y-momentum equation
ε	parameter for turbulent kinetic energy dissipation rate
ϕ	parameter for generalized variable

2. Numerical model

There are two distinct flow regions in the steam surface condenser, i.e. the tube-side and shell-side. The cooling water flows through the tube-side continuously and tube-side flows have been very well studied. Therefore, the focus of the numerical simulation of steam surface condensers is on the shell-side flow and heat transfer. The effect of the tube-side flow on the shell-side flow is through the heat transfer between them. The shell-side fluid is a mixture of vapor, non-condensable gases (mainly air), and liquid. The vapor in the mixture will become condensate due to the heat transfer between the vapor and cooling water that flows on tube-side. The numerical model used in this study includes the effects of turbulence, non-condensable gases, phase change, interphase friction and distributed flow resistance due to tube bundles on the fluid flow and heat transfer on the shell-side of condensers.

Partition plates are commonly used in power plant condensers to support tube bundles. These partition plates restrict the flow in the third direction on the shell-side of the condenser. In addition, the cooling tubes in each sector, which is between the two adjacent partition plates, are relative short. So, the increase in cooling water temperature in each sector is much smaller than the temperature difference between the shell-side fluid and the cooling water. Therefore, the fluid flow in each sector can be assumed two-dimensional. The link between sectors is through the cooling water temperature. Therefore, the quasi-three-dimensional approach suggested by Zhang and Bokil [2] is employed in this study, in which the three-dimensional effect due to the cooling water temperature gradients is taken into account by a series of step by step two-dimensional calculations, each being for one sector. In this study, the numerical model proposed by Zhang and Bokil [2] for the simulation of gas–liquid two-phase flows in condensers, where a constant turbulent viscosity was used, has been extended to include a modified k–ε turbulence model.

2.1. Assumptions

The following assumptions are made in the numerical model:

- The mixture of vapor and air, which is named as the gas-phase, is considered as a perfect gas, the proportions being defined by the air mass fraction.
- Both vapor and liquid condensate are saturated.
- The diffusion terms for the liquid condensate are negligible.
- Pressure is assumed common to both phases.

- The turbulent diffusivity is equal to the turbulent viscosity, i.e., Schmidt number is equal to one.
- Pressure drop from inlet to vent for all sectors must be the same.

2.2. Governing equations

The governing equations for shell-side flow in a condenser are the equations of conservation of mass, momentum for both gas-phase and liquid-phase, and air mass fraction. The general form of the governing equation can be expressed as

$$\frac{\partial}{\partial x}(\beta\rho u\phi)+\frac{\partial}{\partial y}(\beta\rho v\phi)=\frac{\partial}{\partial x}\left(\beta\Gamma_\phi\frac{\partial\phi}{\partial x}\right)+\frac{\partial}{\partial y}\left(\beta\Gamma_\phi\frac{\partial\phi}{\partial y}\right)+S_\phi \tag{1}$$

The expressions for ϕ, Γ_ϕ and S_ϕ are given in Table 1. The pressure correction equation is obtained from the gas-phase continuity equation and gas-phase momentum equations. The liquid volume fraction is obtained from the liquid-phase continuity equation. The gas volume fraction is obtained by using an auxiliary equation.

2.3. Volume fraction

The porous medium concept is used in this study to account for the effect of tube bundles on the fluid flow. The porosity, α, which is employed to describe the flow volume reduction due to tube bundles, is defined as the ratio of the volume occupied by the fluid to the total volume. The gas volume fraction and liquid volume fraction are defined as the ratio of the volume occupied by the gas (vapor and air) to the total volume, and the ratio of the volume occupied by the liquid to the total volume, respectively. Thus,

$$\beta_g+\beta_l=\alpha \tag{2}$$

The porosity, α, is determined by the tube bundle layout. Therefore, the gas volume fraction can be obtained by Eq. (2).

2.4. Distributed resistance

The source terms for the distributed resistance, which is due to tube bundles, are included in the momentum equations for both gas-phase and liquid-phase. They are taken the following forms [2]:

$$(R_x)_m=(\beta\xi_x\rho uU)_m \tag{3}$$

$$(R_y)_m=(\beta\xi_y\rho vU)_m \tag{4}$$

where ξ_x and ξ_y are the pressure loss coefficients and given in [2].

2.5. Interphase friction

The source terms to account for the interphase friction between the gas-phase and liquid-phase are also included in the momentum equations for both phases, which have the following forms [2]:

$$W_{xg}=-W_{xl}=C_{fx}(u_l-u_g) \tag{5}$$

$$W_{yg}=-W_{yl}=C_{fy}(v_l-v_g) \tag{6}$$

where

$$C_{fx}=\frac{1}{2}\rho_g f_d A_d|u_g-u_l| \tag{7}$$

$$C_{fy}=\frac{1}{2}\rho_g f_d A_d|v_g-v_l| \tag{8}$$

$$A_d=\frac{1.5\beta_l}{D_d} \tag{9}$$

The friction factor, f_d, given by Clift et al. [10] is used in this study.

Table 1
Expressions for ϕ, Γ_ϕ and S_ϕ [2]

Equation	ϕ	Γ_ϕ	S_ϕ
Gas-phase continuity equation	1		$-\dot{m}$
Liquid-phase continuity equation	1		$\dot{m}$
Gas-phase x-momentum equation	u^g	μ^{eg}	$\frac{\partial}{\partial x}\left(\beta_g\mu_{eg}\frac{\partial u_g}{\partial x}\right)+\frac{\partial}{\partial y}\left(\beta_g\mu_{eg}\frac{\partial v_g}{\partial x}\right)-\frac{2}{3}\frac{\partial}{\partial x}\left[\beta_g\mu_{eg}\left(\frac{\partial u_g}{\partial x}+\frac{\partial v_g}{\partial y}\right)\right]-\beta_g\frac{\partial p}{\partial x}+W_{xg}-R_{xg}-\dot{m}u_g$
Gas-phase y-momentum equation	v_g	μ_{eg}	$\frac{\partial}{\partial x}\left(\beta_g\mu_{eg}\frac{\partial u_g}{\partial y}\right)+\frac{\partial}{\partial y}\left(\beta_g\mu_{eg}\frac{\partial v_g}{\partial y}\right)-\frac{2}{3}\frac{\partial}{\partial y}\left[\beta_g\mu_{eg}\left(\frac{\partial u_g}{\partial x}+\frac{\partial v_g}{\partial y}\right)\right]-\beta_g\frac{\partial p}{\partial y}+W_{yg}-R_{yg}-\dot{m}v_g$
Liquid-phase x-momentum equation	u_l	0	$-\beta_l\frac{\partial p}{\partial x}+W_{xl}-R_{xl}+\dot{m}u_l$
Liquid-phase y-momentum equation	v_l	0	$-\beta_l\frac{\partial p}{\partial y}+W_{yl}-R_{yl}+\dot{m}v_l+\beta_l\rho_l g$
Air mass fraction equation where $\mu_{eg}=\mu_g+\mu_{tg}$	β_a	$\rho_a D_e$	0.0

2.6. Mass source term

The vapor condensate rate per unit volume, $\dot{m}$, which is the mass source term in the continuity equations for both gas-phase and liquid-phase, is due to the heat transfer between the vapor and cooling water flowing inside the tubes. $\dot{m}$ is calculated by equating the phase change enthalpy with the heat transfer rate from the vapor to the cooling water, i.e.,

$$\dot{m}LV = \frac{T - T_w}{R}A \tag{10}$$

The overall thermal resistance, R, is the sum of all individual thermal resistances obtained from various semi-empirical heat transfer correlations, which are given in [2].

At the vent, the mass source term, $\dot{m}$, is obtained from the global mass balance based on the condensation rate in the tube area and the inlet mass flow rate.

2.7. Turbulence model for gas-phase

Since the diffusion terms for liquid-phase are negligible, the turbulence model is needed for gas-phase only. The turbulence model used in this study is a modified k–ε model with additional source terms for turbulent kinetic energy and its dissipation rate due to distributed resistance and interphase friction. The transport equations for the modified k–ε model have the following forms:

$$\begin{aligned}&\frac{\partial}{\partial x}(\beta_g\rho_g u_g k) + \frac{\partial}{\partial y}(\beta_g\rho_g v_g k)\\ &= \frac{\partial}{\partial x}\left(\beta_g\left(\mu_g + \frac{\mu_{tg}}{\sigma_k}\right)\frac{\partial k}{\partial x}\right) + \frac{\partial}{\partial y}\left(\beta_g\left(\mu_g + \frac{\mu_{tg}}{\sigma_k}\right)\frac{\partial k}{\partial y}\right)\\ &\quad + \beta_g(G - \rho_g\varepsilon) + \frac{1}{3}\beta_g\rho_g k\left(\frac{\partial u_g}{\partial x} + \frac{\partial v_g}{\partial y}\right) + R_k + W_k\end{aligned} \tag{11}$$

$$\begin{aligned}&\frac{\partial}{\partial x}(\beta_g\rho_g u_g \varepsilon) + \frac{\partial}{\partial y}(\beta_g\rho_g v_g \varepsilon)\\ &= \frac{\partial}{\partial x}\left(\beta_g\left(\mu_g + \frac{\mu_{tg}}{\sigma_\varepsilon}\right)\frac{\partial \varepsilon}{\partial x}\right) + \frac{\partial}{\partial y}\left(\beta_g\left(\mu_g + \frac{\mu_{tg}}{\sigma_\varepsilon}\right)\frac{\partial \varepsilon}{\partial y}\right)\\ &\quad + \frac{\beta_g\varepsilon}{k}(C_1 G - C_2\rho_g\varepsilon) + \beta_g\rho_g\varepsilon\left(\frac{\partial u_g}{\partial x} + \frac{\partial v_g}{\partial y}\right) + R_\varepsilon + W_\varepsilon\end{aligned} \tag{12}$$

where $\mu_{tg} = C_\mu\rho_g k^2/\varepsilon$, $\sigma_k = 1.0$, $\sigma_\varepsilon = 1.3$, $C_\mu = 0.09$, $C_1 = 1.44$, $C_2 = 1.92$, and R and W are the additional source terms due to the distributed resistance and interphase friction, respectively.

The tube bundles enhance the production and dissipation of the turbulent kinetic energy. Similar to the turbulent kinetic energy generation at a wall, where the production of the turbulent kinetic energy is the product of the velocity parallel to the wall and the wall shear stress, it is assumed that the source of the turbulent kinetic energy production due to the tube bundles is the rate at which the distributed resistance does work to fluid and the fluid has not had time to provoke viscous thermal heating. Consequently, the turbulent kinetic energy production due to the tube bundles has the following form [11–13]:

$$R_k = R_{xg}|u| + R_{yg}|v| \tag{13}$$

where R_{xg} and R_{yg} are the flow resistance due to tube bundles and given in Eqs. (3) and (4). The turbulent kinetic energy dissipation due to the tube bundles can be expressed as following [10–13]:

$$R_\varepsilon = 1.92\frac{\varepsilon R_k}{k} \tag{14}$$

The production of the turbulent kinetic energy and its dissipation caused by the interphase friction are given as [14]

$$W_k = \beta_g C_{phase}\lfloor W_{xg}(u_l - u_g) + W_{yg}(v_l - v_g)\rfloor \tag{15}$$

$$W_\varepsilon = \frac{C_1\varepsilon}{k}W_k \tag{16}$$

where W_{xg} and W_{yg} are the interphase friction forces and given in Eqs. (5) and (6), and C_{phase} is the interphase exchange coefficient and taken 0.7 here.

Standard wall functions are used to model the effects of walls in the k–ε turbulence model [15,16].

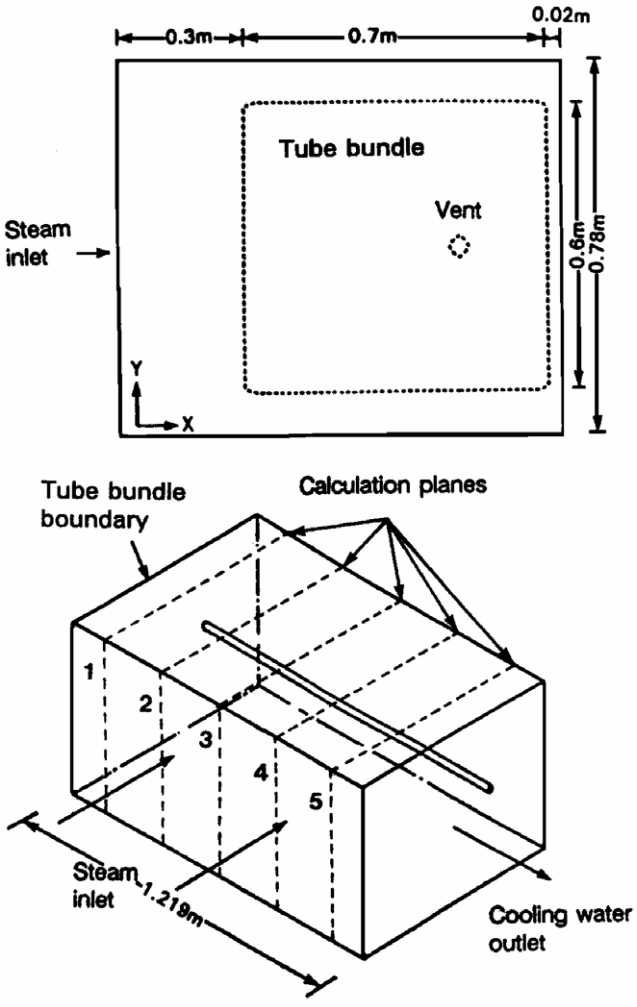

Fig. 1. Configuration of the experimental condenser.

3. Configuration of the experimental condenser

The experimental steam surface condenser presented by Al-Sanea et al. [6] and Bush et al. [8] is used in this study to validate the proposed numerical model. The configuration of this experimental condenser is shown in Fig. 1. The condenser has dimensions of $1.219 \times 0.78 \times 1.02\ m^3$. The tube bundle is composed of 20×20 tubes with equilateral triangular arrangement. The cooling water is arranged to flow in a single pass through the condenser. The gas mixture (vapor and vary small amount of air) flows into the condenser from the inlet located on the left-hand side of the condenser. Air and uncondensed vapor are extracted to the internal vent as shown in the figure. The condensate is removed from the bottom of the condenser. The geometrical and operating parameters are listed in Table 2. The experimental data from this condenser are used to compare with the numerical results to evaluate the predictability of the proposed numerical model.

4. Results and discussion

In this study, the condenser is divided into five sectors along the cooling water flow direction, and the fluid flow in each sector is assumed two-dimensional.

Three different non-uniform grid sizes, 31×34, 46×51 and 62×68, are used for grid-independence test. Table 3 shows the average changes of different variables (pressure, temperature, heat flux and gas-phase velocity magnitude) between different grids. The maximum difference between grids 46×51 and 62×68 is 4.12%. Therefore, the results from the grid 62×68 can be considered as grid independent and the grid 62×68 is used in the simulation.

Table 2
Geometrical and operating parameters

Geometrical parameters	
Condenser length (m)	1.219
Condenser depth (m)	1.02
Condenser height (m)	0.78
Tube outer diameter (mm)	25.4
Tube wall thickness (mm)	1.25
Tube pitch (mm)	34.9
Operating parameters	
Inlet cooling water temperature of (°C)	17.8
Inlet cooling water velocity (m/s)	1.19
Inlet steam pressure (Pa)	27670
Inlet steam flow rate (kg/s)	2.032
Inlet air flow rate (kg/s)	2.48×10^{-4}

Table 3
Average changes in main variables between different grids

Grids	Pressure (%)	Temperature (%)	Heat flux (%)	Velocity (%)
Between 31×34 and 46×51	0.0783	0.0125	4.20	5.98
Between 46×51 and 62×68	0.0322	0.00839	4.12	3.58

4.1. Numerical results

The following discussion is based on the results from Sector #1, and the results from other sectors (#2–#5) are similar.

Fig. 2 shows the numerical results for the gas and liquid velocity vector fields. Since the vapor condenses due to the heat transfer to the cooling water in the tube-side, the amount of vapor decreases greatly. It shows in Fig. 2 that

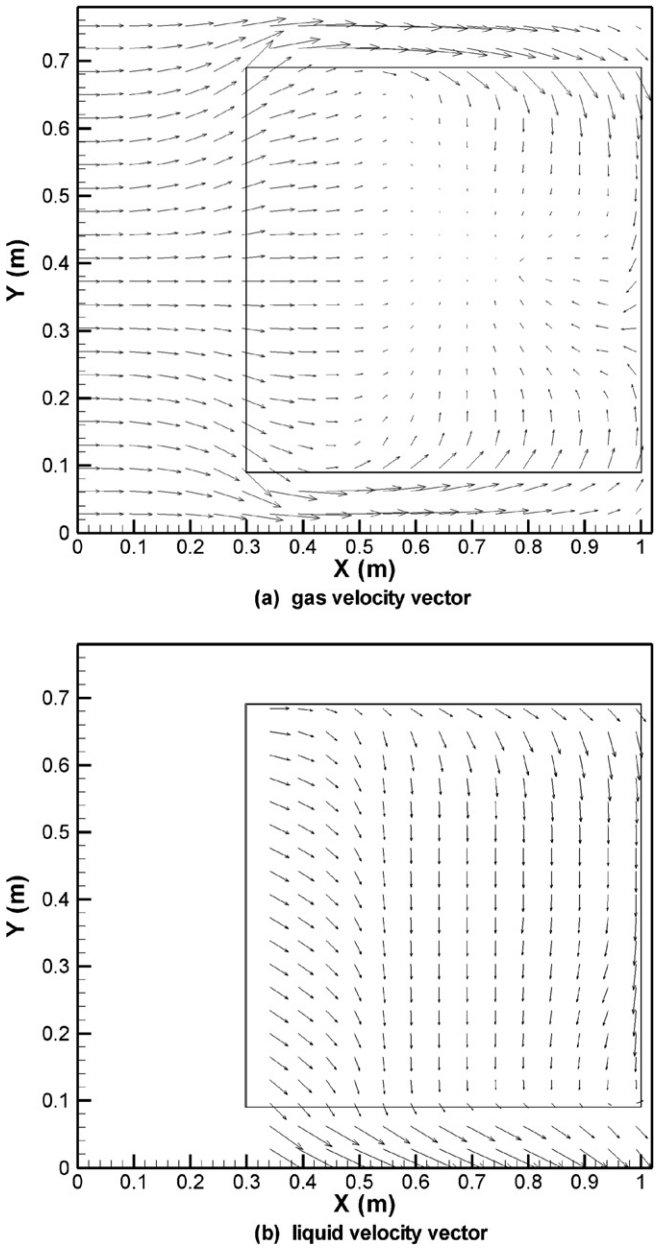

Fig. 2. Velocity vector.

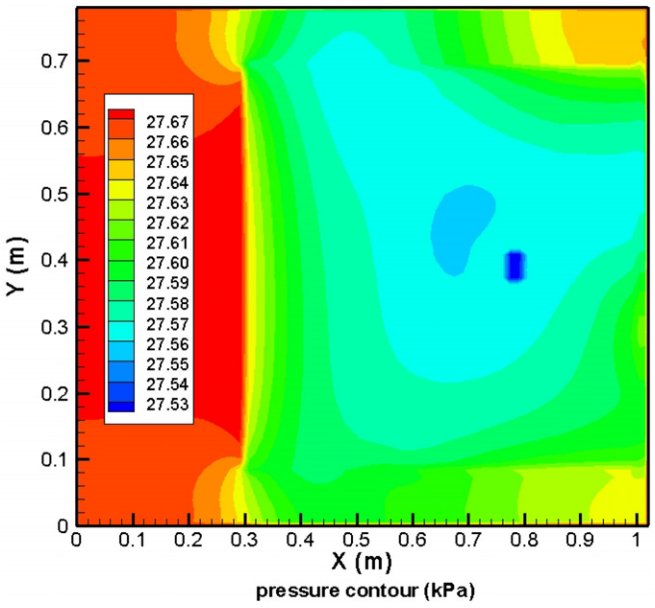

Fig. 3. Pressure contour.

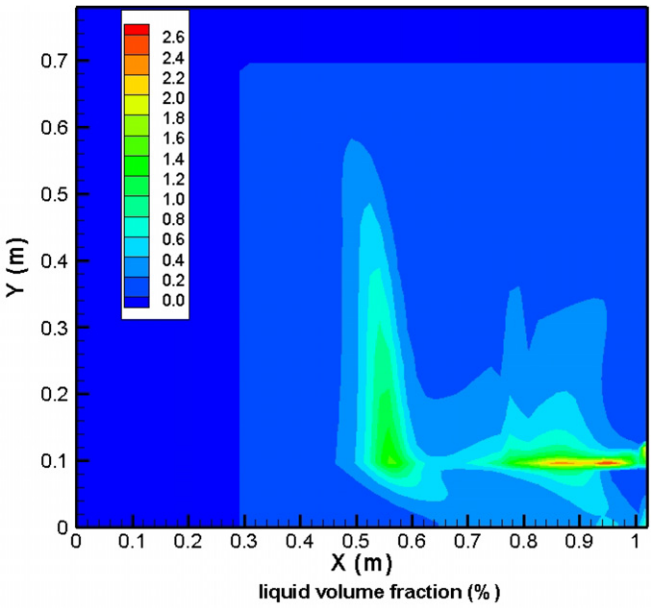

Fig. 5. Liquid volume fraction contour.

the gas-phase velocity decreases as it flows closer to the vent, where non-condensable gases and uncondensed vapor are extracted. At the same time, the liquid appears in the tube bundle. It can be seen from the figure that the liquid flows mainly downwards due to gravity and low gas velocity except at the inlet of the tube bundle and the bottom of the condenser, where gas velocity is high and it is in horizontal direction. The liquid velocity increases as it approaches to the bottom of the condenser where the liquid leaves the condenser. It should be mentioned that the velocity presented in Fig. 2 is the velocity based on the actual flow area of gas and liquid. The increase in the gas velocity when the gas enters the tube bundle is due to the decrease in the porosity in the tube bundle and the increase in liquid velocity at the bottom of the condenser is due to higher gas volume fraction, so lower liquid volume fraction in that region.

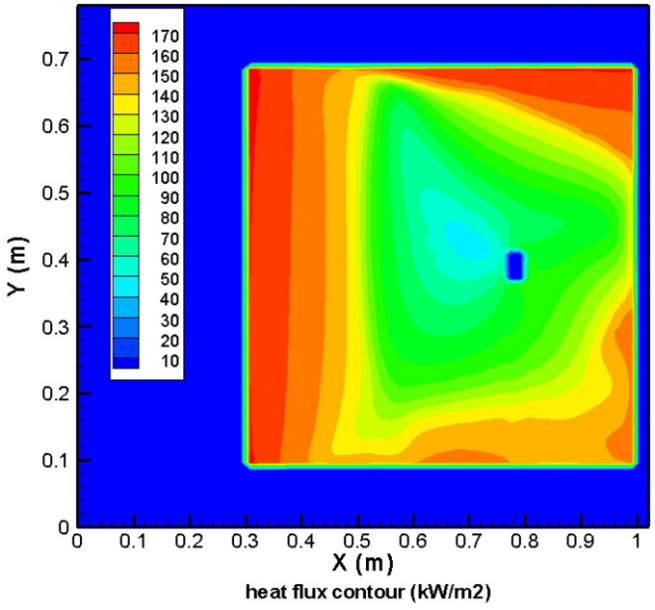

Fig. 4. Average heat flux contour.

Fig. 3 shows the pressure distribution in the condenser. Generally, the pressure at the edge of the tube bundle is higher than that at the center of the tube bundle, which forces the fluid flows towards the vent. Fig. 4 shows the heat flux contour. It can be seen that corresponding with the lower vapor velocity region is the region of lower heat transfer. The highest heat flux is at the entry to the tube bundle, where steam velocities are the highest. The heat flux is high at the periphery of the tube bundle and falls to a low value in the vent area. The liquid volume fraction as shown in Fig. 5 is the highest in the lower part of the tubular region since the amount of liquid is higher there.

4.2. Comparison

Fig. 6 shows the comparison of the average heat flux of the five sectors along different tube row with the experiment data [6,8] and the numerical results when a constant turbulent viscosity was used [2]. Obviously, comparing with the experimental results, the numerical results using the proposed modified k–ε model have some improvement over those without k–ε model except along the 13th row from the bottom of the tube bundles. The 13th row ($y = 0.4654$ m) is located at the center of the tube bundle where the heat flux is lowest. It seems the proposed modified k–ε model over-predicts the turbulent intensity, which leads the higher amount of heat flux at the center of the tube bundles.

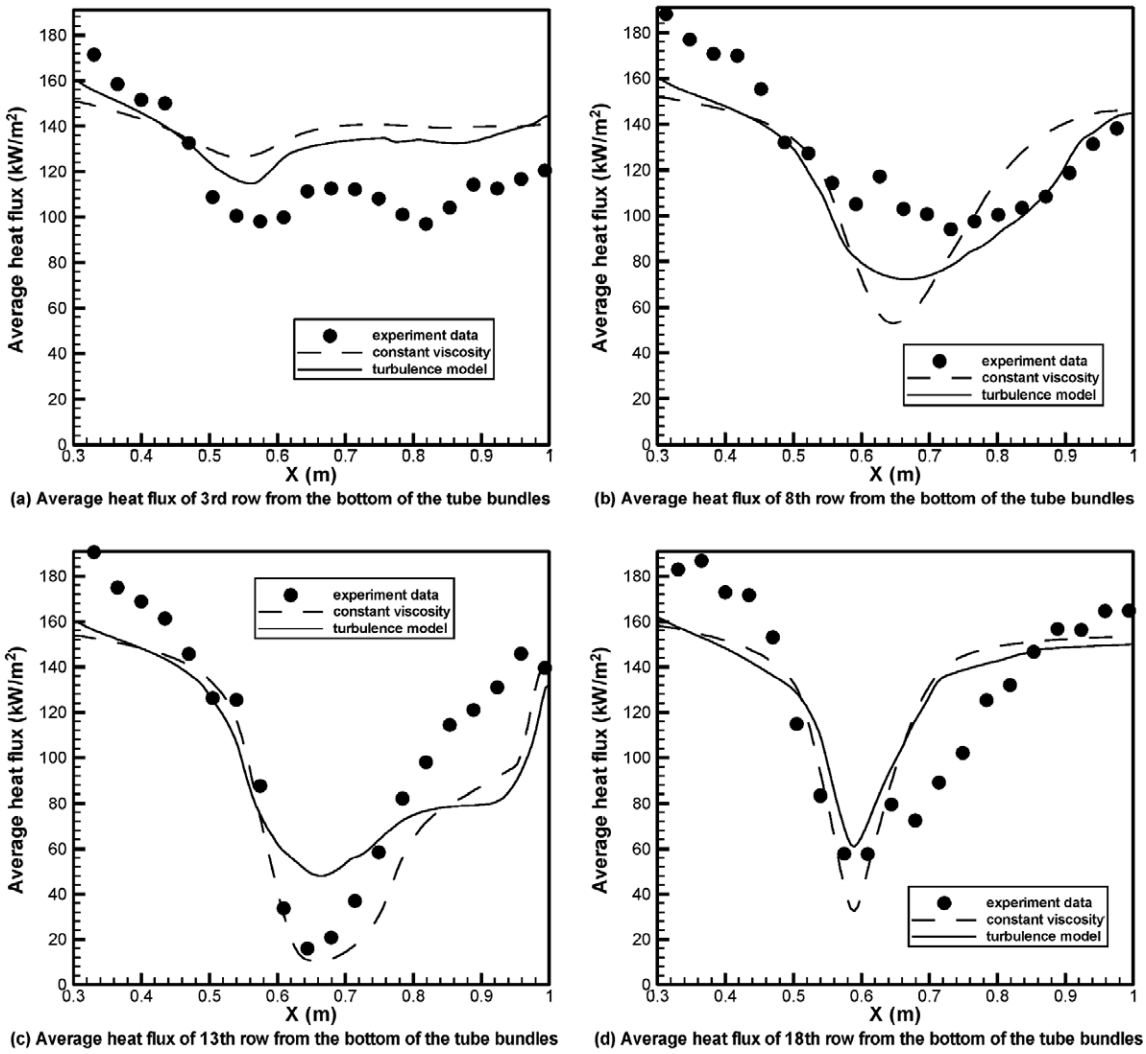

Fig. 6. Comparison of average heat flux.

5. Conclusion

A quasi-three-dimensional two-phase model with modified k–ε turbulence model is applied to simulate the fluid flow and heat transfer in the shell-side of a steam surface condenser and the numerical results are compared with the experimental data. The numerical results agree with the experimental data. They have a better agreement with the experimental data than the numerical results using a constant turbulent viscosity in most regions in the condenser. However, the proposed model over-predicts the heat flux at the center of the tube bundles where the lowest heat transfer rates occur. Therefore, future work is needed to improve the proposed model, which will involve assessment of the effects of closure relationships for condensation, interphase friction forces, non-condensable air and hydraulic resistance of the tube bundle.

References

[1] B.J. Davidson, M. Rowe, Simulation of Power Plant Condenser Performance by Computational Methods: An Overview, Power Condenser Heat Transfer Technology, Hemisphere Publishing Corporation, 1980, pp. 17–49.

[2] C. Zhang, A. Bokil, A quasi-three-dimensional approach to simulate the two-phase fluid flow and heat transfer in condensers, Int. J. Heat Mass Transfer 40 (15) (1997) 3537–3546.

[3] I.S. Ramon, M.P. Gonzalez, Numerical study of the performance of a church window tube bundle condenser, Int. J. Therm. Sci. 40 (2001) 195–204.

[4] M.M. Prieto, I.M. Suarez, E. Montanes, Analysis of the thermal performance of a church window steam condenser for different operational conditions using three models, Appl. Therm. Eng. 23 (2003) 163–178.

[5] R.P. Roy, M. Ratisher, V.K. Gokhale, A computational model of a power plant steam condenser, Trans. ASME J. Energy Resour. Technol. 123 (2001) 81–91.

[6] S.A. Al-Sanea, N. Rhodes, T.S. Wilkinson, Mathematical modeling of two-phase condenser flows, in: Second International Conference on Multi-phase Flow, London, England, 1985, pp. 169–182.

[7] M.R. Malin, Modelling flow in an experimental marine condenser, Int. Commun. Heat Mass Transfer 24 (5) (1997) 597–608.

[8] A.W. Bush, G.S. Marshall, T.S. Wilkinson, The prediction of steam condensation using a three component solution algorithm, in: Proceedings of the Second International Symposium on Condensers and Condensation, University of Bath, UK, 1990, pp. 223–234.

[9] Z.V. Stosic, V.D. Stevanovic, Advanced three-dimensional two-fluid porous media method for transient two-phase flow thermal-hydraulics in complex geometries, Numer. Heat Transfer, Part B 41 (2002) 263–289.

[10] R. Clift, J.R. Grace, M.E. Weber, Bubbles, Drops and Particles, Academic Press, 1978.

[11] M. Prithiviraj, M.J. Andrews, Three-dimensional computer simulation of shell and tube heat exchangers, Heat Transfer Turbulent Flows ASME HTD 318 (1995) 119–127.

[12] M. Prithiviraj, M.J. Andrews, Three dimensional numerical simulation of shell-and-tube heat exchangers. Part I: Foundation and fluid mechanics, Numer. Heat Transfer, Part A 33 (1998) 799–816.

[13] M. Prithiviraj, M.J. Andrews, Three dimensional numerical simulation of shell-and-tube heat exchangers. Part II: Heat transfer, Numer. Heat Transfer, Part A 33 (1998) 817–828.

[14] H.F. Svendsen, H.A. Jakobsen, R. Torvik, Local flow structures in internal loop and bubble column reactors, Chem. Eng. Sci. 47 (13/14) (1992) 3297–3304.

[15] A.K. Majumdar, V.S. Pratap, D.B. Spalding, Numerical computation of flow in rotating ducts, Trans. ASME J. Fluids Eng. 99 (1977) 148–153.

[16] B.E. Launder, D.B. Spalding, The numerical computation of turbulent flows, Comput. Methods Appl. Mech. Eng. 3 (1974) 269–289.